

Article

# Preparation of Maleic Anhydride Grafted Poly(trimethylene terephthalate) (PTT-g-MA) by Reactive Extrusion Processing

Natália F. Braga <sup>1,\*</sup>, Henrique M. Zaggo <sup>1</sup>, Thaís L. A. Montanheiro <sup>2</sup> and Fabio R. Passador <sup>1</sup>

<sup>1</sup> Laboratório de Tecnologia de Polímeros e Biopolímeros, Universidade Federal de São Paulo - UNIFESP, São José dos Campos, SP 12231-280, Brazil; henriquezaggo@gmail.com (H.M.Z.); fabio.passador@unifesp.br (F.R.P.)

<sup>2</sup> Laboratório de Plasmas e Processos, Divisão de Ciências Fundamentais, Instituto Tecnológico de Aeronáutica – ITA, São José dos Campos, SP 12228-900, Brazil; tlamontanheiro@gmail.com

\* Correspondence: natyfbraga@hotmail.com

Received: 5 March 2019; Accepted: 29 April 2019; Published: 4 May 2019



**Abstract:** Maleic anhydride (MA) grafted with poly(trimethylene terephthalate) (PTT)—abbreviated as PTT-g-MA—can be used as a compatibilizing agent to improve the compatibility and dispersion of nanofillers and a dispersed polymer phase into PTT matrix. This work suggests the preparation of PTT-g-MA using a mixture of PTT, MA, and benzoyl peroxide (BPO) by a reactive extrusion process. PTT-g-MA was characterized to confirm the grafting reaction of maleic anhydride on PTT chains by Fourier transform infrared (FTIR) spectroscopy. Thermal properties (differential scanning calorimetry (DSC) and thermogravimetric analysis (TGA)) and rheological analysis (parallel plates rheology) were used to prove the changes that occurred after the graphitization reaction. The reactive processing route allowed the production of the compatibilizing agent (PTT-g-MA) with good thermal properties and with lower viscosity compared to neat PTT, and this could be an alternative for the compatibilization of polymer blends, as example for PTT/ABS (acrylonitrile butadiene styrene) blends and nanocomposites based on PTT matrix.

**Keywords:** poly(trimethylene terephthalate); maleic anhydride; compatibilizing agent

## 1. Introduction

Polymeric blends and nanocomposites have been developed over the years with the aim of creating new materials with desirable features. One of the biggest challenges in this field is the weak interfacial adhesion and poor dispersion of the dispersed phase and/or the filler in the polymeric matrix phase. The low physical attraction forces across the immiscible phase boundaries usually cause immiscible blend systems with weak interfacial adhesion, which have poor mechanical properties. The compatibility between the components has great importance and influence on the final properties of polymer blends and nanocomposites, and the interfacial region that occurs strains transfer from the matrix to the reinforcement agent [1]. The number of immiscible blends is extensive due to the low entropy of mixing two polymers as a result of their long chain structure, and phase separation can occur. This problem has been mitigated since the 1960s with the introduction of small quantities of an additive, known as a compatibilizing agent [2]. The compatibilizing agent is commonly used to improve the compatibility of immiscible polymeric blends. Compatibility is promoted by the presence of functional groups which undergo interaction [3]. These agents graft polymers by reactive reactions, typically using maleic anhydride (MA) or acrylic acid (AA). The introduction of MA has overcome the disadvantage of the low polymer surface energy, improving their surface hydrophilicity and adhesion with polar polymers, inorganic filler, and glass fibers [4].

The compatibilizing agent acts as an organic surfactant, and it is located on the interface between two incompatible polymer phases, where it reduces interfacial tension and promotes adhesion between the phases. The compatibilizer plays an important role in controlling the dispersed phase size in a blend produced in a conventional melt process [3], as the phase becomes smaller and more uniform, there is an increase in the blend stability and, consequently, there is an increase in the mechanical properties.

A variety of substances can be used as compatibilizers for polymer blends, but it is necessary to have structural characteristics of both polymers. For example, block and graft copolymers are commonly used as compatibilizing agents in small percentages in polymer blends, while functionalized polymers are also used as compatibilizing agents [5]. Some works can be found in the literature proposing the use of MA grafting thermoplastic polymers. Montanheiro et al. [1] prepared a compatibilizer by grafting maleic anhydride to poly(hydroxybutyrate-co-hydroxyvalerate) chains by reactive processing using mechanical mixing, as an alternative way to produce polymers with low molecular weight without prejudicing their thermal properties. Hezavehi et al. [6] studied the properties of polypropylene and poly(trimethylene terephthalate) (PP/PTT) blends using maleic anhydride grafted polypropylene (MAPP) as compatibilizer, and the results showed improved adhesion between the phases with the addition of the compatibilizer. Passador et al. [7] studied the influence of two compatibilizers: high-density polyethylene grafted maleic anhydride (HDPE-g-MA), low-linear-density polyethylene grafted maleic anhydride (LLDPE-g-MA), and a mixture of HDPE-g-MA and LLDPE-g-MA on the properties of HDPE/LLDPE/organoclay nanocomposites. The compatibilized nanocomposites with LLDPE-g-MA or a mixture of 50/50 wt% of HDPE-g-MA and LLDPE-g-MA better exhibited the nanoclay's dispersion and distribution with stronger interactions between the matrix and the nanoclay. Xue et al. [8] studied the crystallization behavior of poly(trimethylene terephthalate)/polypropylene (PTT/PP) blends with the addition of polypropylene grafted maleic anhydride (PP-g-MA) as compatibilizer. The shift of PTT's crystallization temperature was larger than that of the PP, suggesting that the addition of PP-g-MA had a greater effect on PTT's crystallization than on PP due to the reaction between MA and PTT.

The current work suggests the development of a new compatibilizing agent, poly(trimethylene terephthalate) grafted maleic anhydride (PTT-g-MA), obtained by a reactive extrusion process. Poly(trimethylene terephthalate) is a polyester belonging to the PET (poly(ethylene terephthalate)) and PBT (poly(butylene terephthalate)) family, but with different physical properties. Due to the odd-numbered methylene groups in its chain, PTT has higher elastic recovery than PET and PBT [9]. PTT can be blended with other polymers in order to develop materials with properties better than those of the original polymers, enhancing the final properties of the material. For instance, Huang [10] prepared PTT/polystyrene (PS) blends, and noted an improvement in tensile strength of the blends compatibilized with styrene-glycidyl methacrylate (SG), which can be attributed to improvement in the interfacial adhesion.

There are few reports in the literature about the melting grafting of PTT-g-MA. Wang and Sun [11] prepared PTT-g-MA from melt reaction to improve the compatibility of blends of cellulose acetate butyrate (CAB) and PTT. The reactive melt mixing was conducted by mixing PTT, MA, and initiator (2,5-dimethyl-2,5-di(tert-butylperoxy) hexane at 240 °C for 5 min at a speed of 100 rpm. They concluded that this compatibilizing agent significantly reduced the phases' sizes, generating strong interfacial interactions and improved mechanical properties. Wu and Liao [12] prepared a mixture of phenol/tetrachloroethane solution (60:40 v/v), MA, and benzoyl peroxide in four equal portions at 2-min intervals to molten PTT to allow grafting to take place. The authors used PTT-g-MA to improve the compatibility and dispersibility of multi-walled carbon nanotubes (MWCNT) within PTT matrix.

In this work, a new route is proposed to obtain PTT-g-MA by reactive extrusion using MA, with benzoyl peroxide as the initiator. Thus, in a single extrusion step, it was possible to obtain a compatibilizing agent with low viscosity and without loss of the thermal properties. The effectiveness of the obtained compatibilizing agent was verified in a PTT/ABS (acrylonitrile butadiene styrene) blend through the analysis of morphology.

## 2. Materials and Methods

### 2.1. Materials

Poly(trimethylene terephthalate) (PTT), with specification Corterra 200, was supplied by Shell Chemicals (Montreal, Canada) with a density of 1.35 g/cm<sup>3</sup>.

Maleic anhydride (MA) with 99% purity was supplied by Sigma-Aldrich (Saint Louis, MO, USA), and the benzoyl peroxide (BPO) initiator was supplied by Dinâmica Química Contemporânea (Indaiatuba, Brazil). Both components were of commercial grade and were used as received. Acrylonitrile butadiene styrene (ABS), with specification MG38 - CYCOLAC, was supplied by SABIC Innovative Plastics (Al Jubail, Saudi Arabia) with a density of 1.04 g/cm<sup>3</sup>.

### 2.2. Reactive Extrusion of PTT-g-MA

Before the reactive processing, PTT was dried at 80 °C for at least 12 h in a vacuum oven to minimize the hydrolytic degradation during processing.

The grafting reaction of MA into PTT chains was carried out by reactive extrusion in a co-rotational twin-screw extruder, AX Plásticos, model AX16:40DR (L/D = 40, D = 16 mm), with a temperature profile of 230/235/235/240/240 °C from the first section to the die, operating at a screw rotation speed of 100 rpm and feeding of 30 rpm. PTT-g-MA was produced with the addition of 96 wt% of PTT, 2 wt% of MA, and 2 wt% of BPO, which was used as the initiator. All components were thoroughly mixed in a bag before extrusion. The extrudate was pelletized and then dried (80 °C for at least 12 h in a vacuum oven) before analysis. The PTT was processed under the same conditions to compare the analyses, and it was labeled as extruded PTT for the polymer after the extrusion process, and neat PTT for the polymer before the extrusion process.

### 2.3. Characterization of the PTT-g-MA

#### 2.3.1. FTIR Spectroscopy

The chemical structures of the MA, PTT, and PTT-g-MA were analyzed by Fourier transform infrared (FTIR) spectroscopy. The samples were analyzed using the PerkinElmer Frontier with a universal attenuated total reflectance (UATR) sensor accessory in the scan range 550–4000 cm<sup>-1</sup>.

#### 2.3.2. Rheological Characterization

The rheological behavior of neat PTT (before extrusion process), extruded PTT (after the extrusion process), and PTT-g-MA was evaluated through viscosity tests as a function of the shear rate (permanent regime) in an inert nitrogen atmosphere at a temperature of 230 °C using a controlled-voltage AR G2 rheometer from TA Instruments. The test geometry was parallel plate, with a plate diameter of 25 mm and a distance between the plates of 1 mm. The deformation applied in each test was defined according to the material, ensuring that the tests were conducted in their regions of linear viscoelastic behavior.

#### 2.3.3. Differential Scanning Calorimetry (DSC)

The thermal properties of neat PTT, extruded PTT, and PTT-g-MA such as glass transition temperature (T<sub>g</sub>), melting temperature<sup>TM</sup>, and crystallization temperature (T<sub>c</sub>) were analyzed by DSC. The DSC tests were performed using Netzsch 204 F1 Phoenix<sup>®</sup> equipment under N<sub>2</sub> atmosphere. Approximately 10 mg of each sample was sealed in an aluminum DSC pan and heated at 10 °C/min under nitrogen atmosphere from 30 to 250 °C kept for 3 min to eliminate the heat history and then cooled to 0 °C. The samples were reheated to 250 °C. The crystallinity degree (X<sub>c</sub>) was calculated using Equation (1):

$$X_c (\%) = \frac{\Delta H_m}{W \cdot \Delta H} \cdot 100, \quad (1)$$

where  $\Delta H_m$  is the total melting enthalpy,  $W$  is the weight fraction of PTT in the sample, and  $\Delta H^\circ$  is the heat of fusion of 100% crystalline PTT, which was taken as 146 J/g [13].

### 2.3.4. Thermogravimetric Analysis (TGA)

The thermal behaviors of neat PTT, extruded PTT, and PTT-g-MA were analyzed by thermogravimetric analysis (TGA) using Netzsch 209 F1 Iris® equipment. Samples were heated from room temperature to 800 °C with a heating rate of 10 °C min<sup>-1</sup>, under nitrogen atmosphere.

### 2.3.5. Verification of the effectiveness of the PTT-g-MA in the phase formation of the PTT/ABS blend

The PTT/ABS (60/40) and PTT/PTT-g-MA/ABS (57/3/40) blends were prepared in a co-rotational twin-screw extruder, AX Plásticos, model AX16:40DR (L/D = 40, D = 16 mm), with temperature profile of 230/235/240/240/240 °C from the first section to the die, operating at screw rotation speed of 120 rpm and feeding of 30 rpm. Samples were prepared in a mini injector (Thermo Scientific Haake MiniLab) with an average temperature of 260 °C. The fracture surfaces of the blends were coated with a thin layer of gold and were analyzed by scanning electron microscopy (SEM) FEI Nova NanoSEM 450, operating at 2 kV.

## 3. Results and Discussion

### 3.1. Grafting Mechanism Between PTT and MA

Figure 1 illustrates the reaction mechanism proposed for MA grafting PTT chains. The grafting reaction of PTT occurs in three stages: (1) Benzoyl peroxide (BPO) breaks into two alkoxy radicals upon heating. (2) The radical then extracts hydrogen atoms from the backbone of the molten polymer to generate the macromolecular radicals—alkyl radical. (3) The alkyl radical initiates the grafting of the vinyl groups of maleic anhydride (MA), producing the compatibilizer PTT-g-MA [11]. These reaction steps occur simultaneously in the extruder. The reactions start at the feed zone, supported by the temperature of the equipment and by the friction of the particles (viscous heating) and continue through the plastification zone.

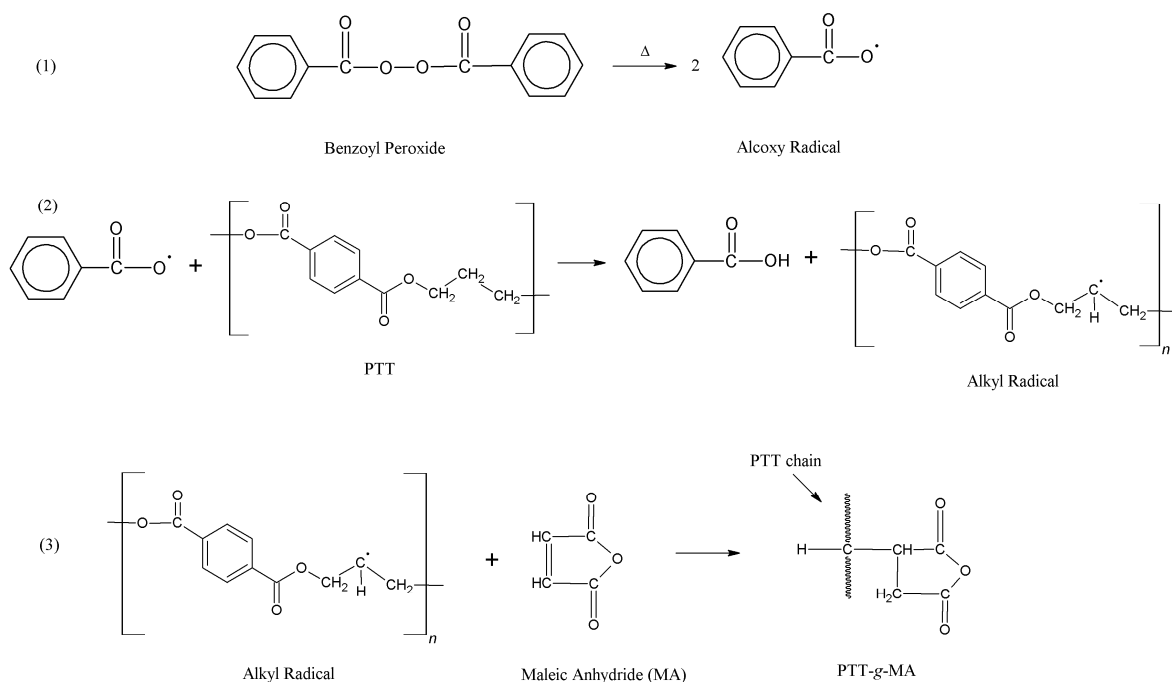


**Figure 1.** Reaction mechanism of maleic anhydride (MA) in poly(trimethylene terephthalate) (PTT) chains in the presence of benzoyl peroxide (BPO). PTT-g-MA: MA grafted with PTT.

### 3.2. FTIR Spectroscopy

In order to confirm the grafting of MA onto PTT chains, the samples were characterized by FTIR spectroscopy, as this technique enables the determination of the molecular composition and structure of solid, liquid, and even gaseous samples [14]. The spectra in the region of 550–4000  $\text{cm}^{-1}$  of MA, extruded PTT, and PTT-g-MA are shown in Figure 2, even as a zoomed-in view of the region between 1600 and 1900  $\text{cm}^{-1}$ , allowing the identification of the peaks resulting from the grafting reaction. It was observed that all the characteristic bands of extruded PTT could also be observed in the PTT-g-MA spectrum. The intense band at 1710  $\text{cm}^{-1}$  was related to the stretch of the carbonyl group ( $\text{C}=\text{O}$ ) characteristic of PTT. Vibrational bands of PTT are associated with the terephthalate ring and the trimethylene group [15]. The band at 1245  $\text{cm}^{-1}$  was attributed to the ester group, whereas the band at 2958  $\text{cm}^{-1}$  was attributed to aromatic CH groups, both resulting from the terephthalate groups [16]. The wavenumber at 723  $\text{cm}^{-1}$  corresponds to coupled vibration of the carbonyl out-of-plane ring deformation of the phenyl group [17].

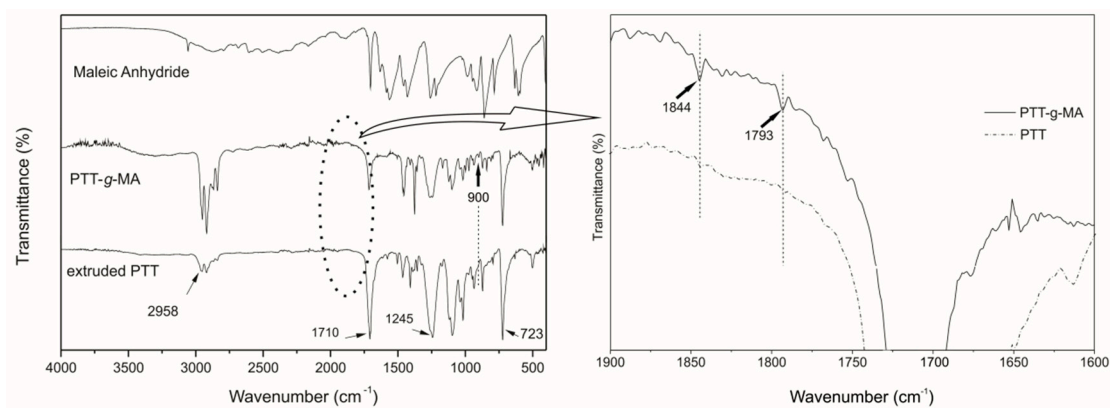


**Figure 2.** FTIR spectra of maleic anhydride, PTT-g-MA, and extruded PTT (left) and zoom at region between 1900–1600  $\text{cm}^{-1}$  (right).

It is expected that the reactions between OH, COOH, and ester groups from MA modified the PTT chains [18]. In this way, the MA grafting on PTT chains was confirmed by the appearance of two new absorption bands in the region between 1600 and 1900  $\text{cm}^{-1}$ , highlighted in Figure 2. The two new bands, one at 1844 and the other at 1793  $\text{cm}^{-1}$ , are related to the symmetric and asymmetric stretching of the carbonyl groups from the grafted MA, present in the PTT-g-MA structure [11,12]. A new band at 900  $\text{cm}^{-1}$  was also observed on the PTT-g-MA spectrum, indicating the stretching of anhydride CO [19] and confirming the reaction between PTT and MA.

### 3.3. Rheological analysis

The rheological analysis was measured in order to characterize the melt viscoelasticity of PTT before and after extrusion process (neat PTT and extruded PTT, respectively), and PTT-g-MA. Figure 3 shows the viscosity dependence concerning the shear rate of the samples at 230 °C. The neat PTT presented initial viscosity ( $\eta_0$ ) value around 446 Pa.s while extruded PTT showed  $\eta_0$  around 370 Pa.s and PTT-g-MA around 330 Pa.s. The  $\eta_0$  was measured at the shear rate of 0.01  $\text{s}^{-1}$ . The value of  $\eta_0$  can be correlated with the molar mass of the material, since smaller molar masses are related to lower melt viscosity. It is noted that the extrusion process decreases the  $\eta_0$  of extruded PTT, related to chain breaking, however, this change is not significant. Comparing PTT-g-MA with neat PTT, a more significant decrease can be observed, which may be related to chain breaking during processing, as well as breaking of chains resulting from graphitization reactions, since this process is an exothermic process and can increase the local temperature, contributing to the breaking of chains. However, the viscosity of neat PTT and extruded PTT are nearly unchanged with increasing shear rate, showing characteristics of a Newtonian fluid. Extruded PTT had a lower viscosity, comparing to PTT before extrusion, due to

chain breakage during the processing. It can also be observed that at low shear rate range, the viscosity of PTT-g-MA did not change, while at higher shear rate, the viscosity decreases sharply with increasing shearing rate, exhibiting pseudoplastic behavior, i.e., viscosity decreases gradually with increasing shear rate, due to the disentanglements between the molecular chains, occurred during the reactive processing. This feature can be essential for the compatibilization process. Since this compatibilizer agent has a lower viscosity in the melt, it may interact more intensively with the other components of the mixture during processing. However, it is necessary to know the thermal parameters, so that premature degradation of this component does not occur.

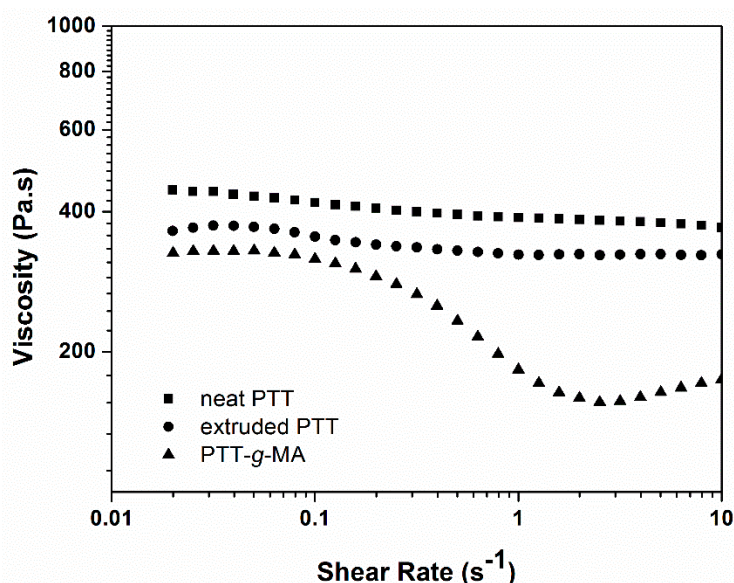


**Figure 3.** Viscosity curve as a function of the shear rate obtained by deformational rheometry of PTT, extruded PTT and PTT-g-MA.

#### 3.4. Thermal Analysis: DSC and TGA

The thermal properties of neat PTT, extruded PTT, and PTT-g-MA were analyzed by DSC. The first heating, cooling, and the second heating scans are shown in Figure 4 a–c, respectively. The glass transition temperature ( $T_g$ ), melting temperature ( $T_m$ ), melting enthalpy ( $\Delta H_m$ ), crystallization temperature ( $T_c$ ), and the degree of crystallinity ( $X_c$ ) are described in Table 1.

In Figure 4a it is observed that neither the extrusion process nor the incorporation of MA changed the  $T_m$  of neat PTT, which was around 227 °C. The  $T_g$  of PTT is difficult to detect by heating PTT with a linear heating rate [20,21], and it depends on the polymer's crystallinity. In this work, careful analysis showed that the  $T_g$  was obtained only by the first heating scan (Figure 4a). The  $T_g$  of neat PTT was 67.2 °C.  $T_g$  was not evident for extruded PTT or PTT-g-MA using the DSC technique. Because  $T_g$  corresponds to variations in the heat capacity due to chain mobility, it can be concluded that after extrusion processing, the heat capacity became smaller compared to neat PTT [22]. Moreover, the chain elasticity is an important factor that influences in the  $T_g$ —once there are large side groups in the backbone of the polymer, the chain elasticity of the polymer decreases [23].

From the cooling scans in Figure 4b, it can be observed that the addition of MA into PTT chains decreased the  $T_c$  from 180 °C in extruded PTT to 173 °C in the PTT-g-MA compatibilizer. The crystallization peak for extruded PTT was narrower than those of neat PTT or PTT-g-MA, indicating the formation of crystals with more homogeneous size distribution and allowing polymer crystal organization. Zhang et al. [24] compared raw PTT resin to kneaded PTT and observed that  $T_c$  values became higher and the crystallization peak became much narrower, meaning that the crystallization rate of PTT was greatly improved through the extrusion process. This behavior was

confirmed by the degree of crystallinity, which considerably increased compared to the neat and extruded PTT.

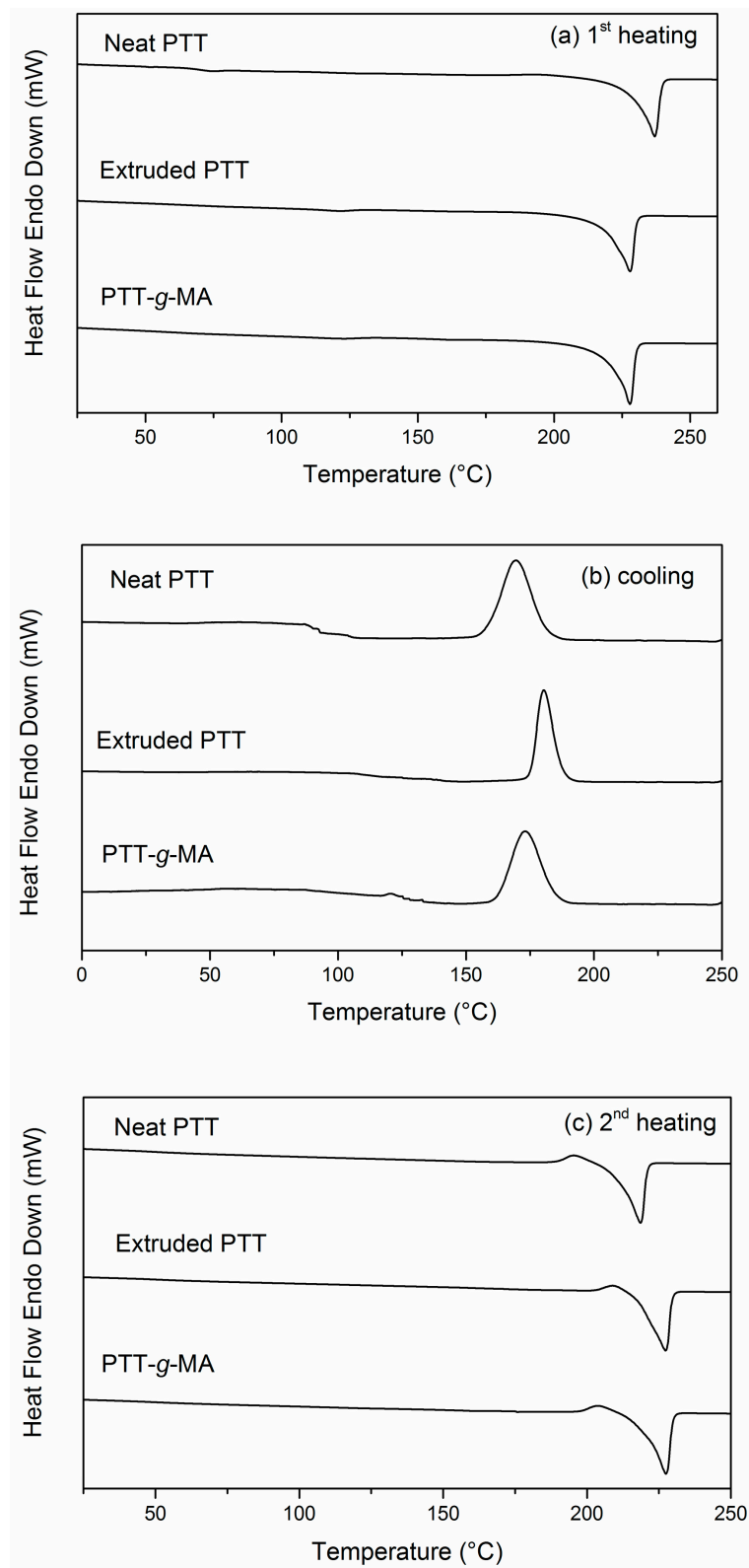


**Figure 4.** DSC thermograms for neat PTT, extruded PTT, and PTT-g-MA: (a) first heating, (b) cooling, and (c) second heating.

**Table 1.** Thermal properties obtained by DSC analysis.

First Heating				
Sample	T <sub>g</sub> (°C)	T <sub>m1</sub> (°C)	ΔH <sub>m1</sub> (J/g)	X <sub>c1</sub> (%)
Neat PTT	67.2	227	64.3	44.1
Extruded PTT	-	227	55.4	37.9
PTT-g-MA	-	227	59.5	42.4
Cooling				
Sample	T <sub>c</sub> (°C)			
Neat PTT	170			
Extruded PTT	180			
PTT-g-MA	173			
Second Heating				
Sample	T <sub>m2</sub> (°C)	ΔH <sub>m2</sub> (J/g)	X <sub>c2</sub> (%)	
Neat PTT	228	64.0	43.8	
Extruded PTT	227	60.6	41.5	
PTT-g-MA	227	64.2	45.8	

T<sub>m</sub> showed no significant changes during the second heating scan (Figure 4c), and it was not possible to observe the T<sub>g</sub>. The glass transition temperature is defined as the temperature at which the amorphous phase becomes mobile, and a change in the heat capacity is observed with this event. In the second heating, it was not possible to determine the T<sub>g</sub>, probably due to an extensive broadening of the change in baseline, meaning that the amorphous phase was smaller in this case compared to the first heating scan. This behavior was justified, because there was previous controlled chain crystallization in the cooling scan [22].

PTT is a typical semicrystalline polymer, and grafting reaction may cause changes in its structure. It is possible to observe that MA did not inhibit the crystal formation process, but increased the degree of crystallinity in the second heating, as observed in Table 1. X<sub>c1</sub> and X<sub>c2</sub> for neat PTT were very close. However, the X<sub>c2</sub> was higher than X<sub>c1</sub> for both extruded PTT and PTT-g-MA because, during the controlled cooling in the DSC analysis, the polymer chain was able to organize and form more crystals. X<sub>c1</sub> reflects the crystals formed during the material processing with no controlled cooling rate.

The thermal properties of neat PTT, extruded PTT, and PTT-g-MA were also analyzed by TGA. Figure 5 shows that the samples had similar thermal decomposition patterns, and the thermal degradation occurred in a single-step process. The values of initial degradation temperature (T<sub>onset</sub>), the degradation temperature of 10% and 50% of weight loss, and the maximum weight-loss rate temperature (T<sub>max</sub>) obtained from the first derivative of the curve are shown in Table 2. Extruded PTT polymer underwent thermal degradation, T<sub>onset</sub>, at 387 °C, the neat PTT at 388 °C, and PTT-g-MA at 378 °C. Grafting MA into PTT chains did not vary the degradation pattern, since T<sub>10%</sub> and T<sub>50%</sub> underwent minor shifts but remained very close for PTT-g-MA, neat PTT, and extruded PTT. The T<sub>max</sub> values were also almost the same for all of them, indicating that MA did not change the maximum weight loss degradation behavior of extruded PTT. In general, it can be said that the addition of MA did not alter the thermal stability of PTT polymer. Thus, the compatibilizing agent was not degraded during its processing, according to the TGA curves.

**Table 2.** Initial thermal degradation temperature (T<sub>onset</sub>), temperatures at weight loss of 10% and 50%, and maximum weight loss rate temperature (T<sub>max</sub>).

Sample	T <sub>onset</sub> (°C)	T <sub>10%</sub> (°C)	T <sub>50%</sub> (°C)	T <sub>max</sub> (°C)
Extruded PTT	387	385	409	407
Neat PTT	388	389	411	408
PTT-g-MA	378	379	405	405

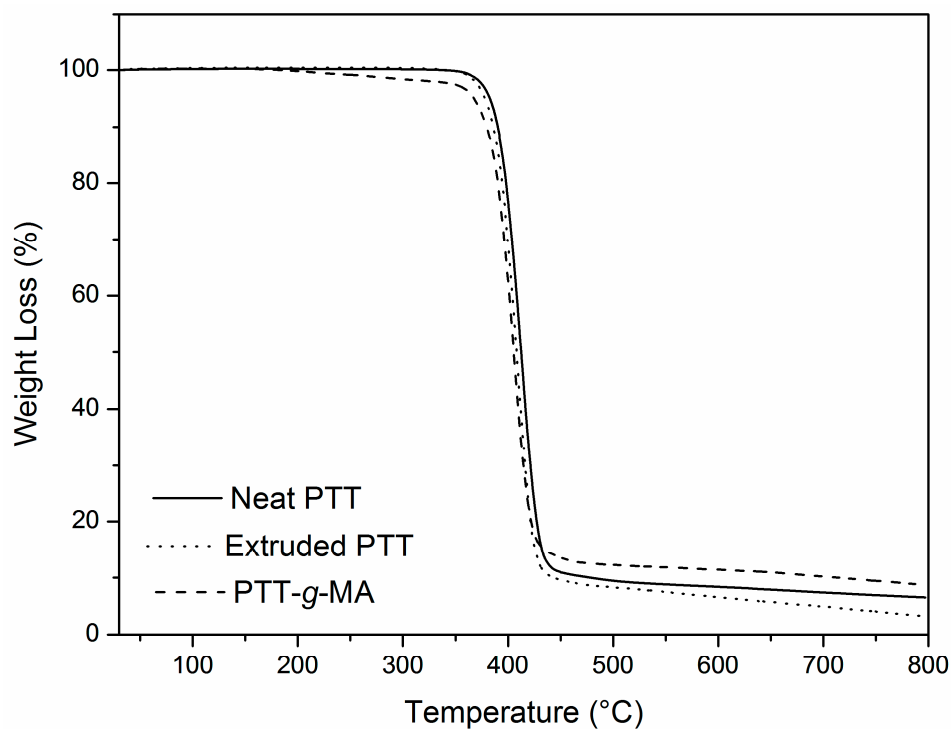


**Figure 5.** Thermal degradation behavior of neat PTT, extruded PTT, and PTT-g-MA.

### 3.5. Effectiveness of PTT-g-MA as a Compatibilizer for PTT/ABS Blend

Figure 6 shows the effect of adding PTT-g-MA in the PTT/ABS blend. To show the evidence of the enhancement properties of PTT using PTT-g-MA, we prepared a PTT/ABS (60/40) blend and a PTT/PTT-g-MA/ABS (57/3/40) blend using the extrusion process. The addition of a compatibilizer in an incompatible blend usually results in finer and more stable morphology, better processability, and improved mechanical properties. Through SEM analysis of the fracture surface, it was possible to note that the morphologies of the blends with and without the compatibilizing agent were quite different. In Figure 6a it is possible to observe the presence of ABS domains in the PTT matrix. The domains are marked in the image for better visualization. The domain consisted of a matrix of styrene acrylonitrile (SAN) and polybutadiene (PB) dispersed in the SAN matrix. As seen in Figure 6b, the addition of 3 wt% of PTT-g-MA in the system reduced the particle size of these domains. The compatibilizer acted on the morphological formation of the PTT/ABS blends. During the melt mixing, the flow of the extruder made the compatibilizing agent go to the extremity of the PTT, causing a gradient in the interfacial tension along the surface of the ABS phase, favoring the “tip streaming” mechanism. In this way, the ABS phase coalescence was suppressed, and this was caused by the immobilization of the interface due to the interfacial tension gradient or elastic repulsion resulting from the compression of the chains of the compatibilizer. As a result, there was a decrease in the size of the second phase (ABS). It is thus possible to conclude that the compatibilizing agent acted in the suppression of ABS phase coalescence during the melt processing, reducing the phase size of the ABS in the PTT/PTT-g-MA/ABS (57/3/40) blend. Thus, with these results, it is possible to check the effectiveness of PTT-g-MA as a compatibilizing agent for the PTT/ABS blends.

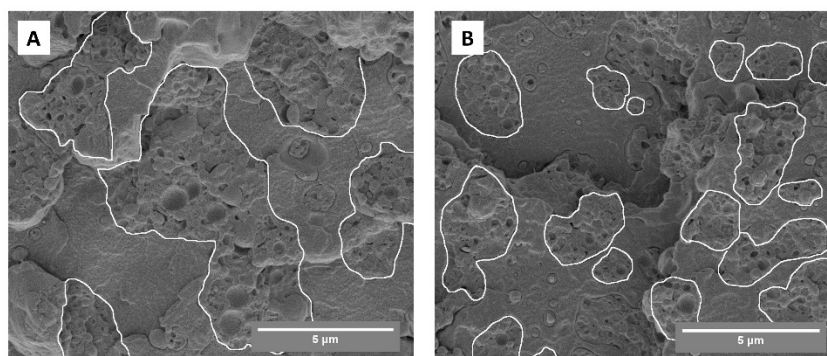


**Figure 6.** SEM images of PTT/ABS blends (A) without and (B) with compatibilizing agent.

#### 4. Conclusions

This paper proposed a new route to produce a compatibilizing agent by grafting maleic anhydride (MA) into poly(trimethylene terephthalate) (PTT) chains by reactive processing. The poly(trimethylene terephthalate) grafted maleic anhydride (PTT-g-MA) showed lower viscosity compared to neat PTT and extruded PTT, and the thermal analysis results showed that MA did not have a significant impact on the thermal degradation of PTT. Thus, the PTT-g-MA showed good thermal and rheological properties, making it an excellent candidate for use as a compatibilizer in polymer blends and nanocomposites using PTT as a polymer matrix. The effectiveness of this compatibilizer was tested on PTT/ABS blends, where the addition of PTT-g-MA decreased the size of the ABS phase compared to the non-compatibilized blend.

**Author Contributions:** Conceptualization, N.F.B., H.M.Z., T.L.A.M. and F.R.P.; Data curation, N.F.B., H.M.Z., T.L.A.M. and F.R.P.; Methodology, N.F.B., H.M.Z., T.L.A.M. and F.R.P.; Supervision, F.R.P.; Validation, F.R.P.; Visualization, F.R.P.; Writing—original draft, N.F.B., T.L.A.M. and F.R.P.; Writing—review & editing, N.F.B., T.L.A.M. and F.R.P.

**Funding:** The authors would like to thank the Brazilian Funding Institutions CAPES (Coordenação de Aperfeiçoamento de Pessoal de Nível Superior – Brasil - 001), CNPq (Conselho Nacional de Desenvolvimento Científico e Tecnológico – Process 405675/2018-6 and 310196/2018-3), and FAPESP (Fundação de Amparo à Pesquisa do Estado de São Paulo - Process 2016/19978-9 and 2017/24873-4) for financial support. And NSF grant #1126100.

**Acknowledgments:** The authors would like to thank the SEM images which was performed in part at the Biosciences Electron Microscopy Facility of the University of Connecticut (USA).

**Conflicts of Interest:** The authors declare no conflict of interest.

#### References

1. Montanheiro, T.L.D.A.; Passador, F.R.; Oliveira, M.P.D.; Durán, N.; Lemes, A.P. Preparation and Characterization of Maleic Anhydride Grafted Poly(Hydroxybutyrate-co-Hydroxyvalerate) – PHBV-g-MA. *Mater. Res.* **2016**, *19*, 229–235. [[CrossRef](#)]
2. Chen, C.C.; White, J.L. Compatibilizing Agents in Polymer Blends: Interfacial Tension, Phase Morphology, and Mechanical Properties. *Polym. Eng. Sci.* **1993**, *33*, 923–930. [[CrossRef](#)]
3. Gaylord, N.G. Compatibilizing Agents: Structure and Function in Polyblends. *J. Macromol. Sci. Part A - Chem.* **1989**, *26*, 1211–1229. [[CrossRef](#)]
4. Rzaev, Z.M.O. Graft Copolymers of Maleic Anhydride and Its Isostructural Analogues: High Performance Engineering Materials. *Int. Rev. Chem. Eng.* **2011**, *3*, 153–215.
5. Al-Malaika, S.; Axtell, F.; Rother, R.; Gilbert, M. Additives for Plastics. In *Brydson's Plastics Materials*; Gilbert, M., Ed.; Elsevier Science: Amsterdam, The Netherlands, 2016; pp. 127–168.
6. Hezavehi, E.; Bigdeli, A.; Zolgharnein, P. Morphological, thermal and mechanical properties of nanostructured materials based on polypropylene/poly (trimethylene terephthalate) blended fibers and organoclay. *Mater. Sci. Pol.* **2012**, *30*, 82–91. [[CrossRef](#)]

7. Passador, F.R.; Ruvolo-Filho, A.C.; Pessan, L.A. Effects of different compatibilizers on the rheological, thermomechanical, and morphological properties of HDPE/LLDPE blend-based nanocomposites. *J. Appl. Polym. Sci.* **2013**, *130*, 1726–1735. [[CrossRef](#)]
8. Xue, M.L.; Yu, Y.L.; Chuah, H.H. Reactive compatibilization of poly(trimethylene terephthalate)/polypropylene blends by polypropylene-graft-maleic anhydride. Part 2. Crystallization behavior. *J. Macromol. Sci. Part B Phys.* **2007**, *46*, 603–615. [[CrossRef](#)]
9. Wu, T.; Li, Y.; Wu, Q.; Song, L.; Wu, G. Thermal analysis of the melting process of poly(trimethylene terephthalate) using FTIR micro-spectroscopy. *Eur. Polym. J.* **2005**, *41*, 2216–2223. [[CrossRef](#)]
10. Huang, J. Polymer Blends of Poly (trimethylene terephthalate) and Polystyrene Compatibilized by Styrene-Glycidyl Methacrylate Copolymers. *J. Appl. Polym. Sci.* **2003**, *88*, 2247. [[CrossRef](#)]
11. Wang, D.; Sun, G. Novel Polymer Blends from Polyester and Bio-Based Cellulose Ester. *J. Appl. Polym. Sci.* **2011**, *119*, 2302–2309. [[CrossRef](#)]
12. Wu, C.S.; Liao, H.T. Characterization and antistatic behavior of SiO<sub>2</sub>-functionalized multiwalled carbon nanotube/poly(trimethylene terephthalate) composites. *J. Polym. Res.* **2013**, *20*, 253. [[CrossRef](#)]
13. Szymczyk, A.; Paszkiewicz, S.; Roslaniec, Z. Influence of intercalated organoclay on the phase structure and physical properties of PTT-PTMO block copolymers. *Polym. Bull.* **2013**, *70*, 1575–1590. [[CrossRef](#)]
14. Tolstoy, V.P.; Chernyshova, I.V.; Skryshevsky, V.A. *Handbook of Infrared Spectroscopy of Ultrathin Films*; John Wiley and Sons: Hoboken, NJ, USA, 2003.
15. Yamen, M.; Ozkaya, S.; Vasanthan, N. Structural and Conformational Changes During Thermally-Induced Crystallization of Poly(trimethylene terephthalate) by Infrared Spectroscopy. *J. Polym. Sci. Part B Polym. Phys.* **2008**, *46*, 1497–1504. [[CrossRef](#)]
16. Farahani, M.F.; Jafari, S.H.; Khonakdar, H.A.; Yavari, A.; Melati, A. FTIR and Thermal Analyses of Intermolecular Interactions in Poly(trimethylene terephthalate)/Phenoxy Blends. *Polym. Eng. Sci.* **2011**, *51*, 518–525. [[CrossRef](#)]
17. Al-omairi, L.M. Crystallization, Mechanical, Rheological and Degradation Behavior of Polytrimethylene Terephthalate, Polybutylene Terephthalate and Polycarbonate Blend. Ph.D. Thesis, RMIT University, Melbourne, Australia, 2010.
18. Bai, Y.; Li, N.; Liu, Y.; Run, M. Morphology and Mechanical Properties of Poly(trimethylene terephthalate)/Maleinized Acrylonitrile-Butadiene-Styrene Blends. *Asian J. Chem.* **2015**, *27*, 2548–2554. [[CrossRef](#)]
19. Smith, A.L. *Applied Infrared Spectroscopy: Fundamentals, Techniques, and Analytical Problem-Solving*; Smith, A.L., Ed.; John Wiley & Sons: Chichester, UK, 1979.
20. Sarathchandran, C.; Chan, C.H.; Abdul Karim, S.R.; Thomas, S. Poly(trimethylene terephthalate) – The New Generation of Engineering Thermoplastic Polyester. In *Physical Chemistry of Macromolecules: Macro to Nanoscales*; Chan, C.H., Chia, C.H., Thomas, S., Eds.; Apple Academic Press: Palm Bay, FL, USA, 2014; pp. 573–618.
21. Pyda, M.; Boller, A.; Grebowicz, J.; Chuah, H.; Lebedev, B.V.; Wunderlich, B. Heat Capacity of Poly (trimethylene terephthalate). *J. Polym. Sci. Part B Polym. Phys.* **1998**, *36*, 2499–2511. [[CrossRef](#)]
22. Montanheiro, T.L.D.A.; Cristóvan, F.H.; Machado, J.P.B.; Tada, D.B.; Durán, N.; Lemes, A.P. Effect of MWCNT functionalization on thermal and electrical properties of PHBV/MWCNT nanocomposites. *J. Mater. Res.* **2015**, *30*, 55–65. [[CrossRef](#)]
23. Boztuğ, A.; Basan, S. The modification and characterization of maleic anhydride-styrene-methyl methacrylate terpolymer by poly(ethylene adipate). *J. Mol. Struct.* **2007**, *830*, 126–130. [[CrossRef](#)]
24. Zhang, J. Study of Poly (trimethylene terephthalate) as an Engineering Thermoplastics Material. *J. Appl. Polym. Sci.* **2004**, *91*, 1657–1666. [[CrossRef](#)]

